ELSEVIER

Seminars in
ROENTGENOLOGY

Orbital Implants: Normal Imaging Appearance, Pitfalls and Complications

Ilona M. Schmalfuss, MD,[*,1], Jake Davenport, MD,[†,*,1] and Matthew E. Harris, MD[‡,*,1]

Introduction

In the past decades, there has been an explosion in the use of orbital implants and devices due to an aging population and technical advancements, with many patients having more than 1 implant/device in place. Cataracts account for the majority of placed implants with 24.4 million Americans receiving an artificial lens in 2010 and a projected rise to 50.2 million in 2050.[1] Similar trends are seen with some of the newer devices such as glaucoma drainage pumps with an increase of 184% between 1995 and 2004 in Medicare patients alone, with more widespread use expected with continued improvements in device technology and surgical techniques.[2]

As with the majority of surgical procedures, complications can occur. These are mostly detected by an ophthalmologic examination with only a few patients requiring dedicated orbital imaging. Nevertheless, with the increasing frequency of orbital implant and device placements, it is very likely radiologists will encounter these devices on a daily basis as the majority of routine brain, maxillofacial, and neck CT and MRI studies include the orbital structures within the scanned volume. Therefore, it is critical for the radiologist to be familiar with imaging findings of common orbital implants and devices. This article provides a review of the normal appearance of orbital implants and devices, potential complications and their mimics as applicable to facilitate accurate diagnosis and timely treatment of complications as well as to prevent potentially unnecessary, invasive surgery in some patients.

*University of Florida, Gainesville, FL.
†Medical Center Radiology Group, Orlando, FL.
‡Radiology Partners MBB Radiology, Jacksonville, FL.
Conflict of interest: None.
Address reprint requests to Ilona M. Schmalfuss, MD, University of Florida, 1600 SW Archer Road, PO Box 100374, Gainesville, FL 32610. E-mail: schmai@radiology.ufl.edu
[1]NF/SG Veterans Health Administration.

Intraocular Lens Replacement

Cataracts are acquired lens opacities leading to refractive defects in the lens. Worldwide, cataracts are the most common cause of treatable blindness affecting more than 68% of individuals 80 years or older.[1] Cataracts are typically treated with an intraocular lens replacement with the pseudophakic surgical method being most commonly used. In this technique, the native lens is first removed by emulsification before the intraocular artificial lens is placed. The pseudophakic intraocular lens has 2 components: the optic part is refractive and the haptic portion holds the optic part in place by attaching to the native lens capsule. Currently, acrylic is the most commonly used artificial lens material, whereas previously polymethylmethacrylate and silicone intraocular lenses were prevalent.[3]

Normal Imaging Appearance

The native lens is biconvex ellipsoid in shape. It is contained within a thin capsule and held in place by suspensory ligaments at the plane of the iris. It is best visualized on CT and T2-weighted images due to significant attenuation difference with the adjacent aqueous and vitreous humor (Fig. 1).[4] A pseudophakic intraocular lens should be in the same position as the native lens as it was surgically placed into the native lens capsule. In contrast to the native lens, the pseudophakic lens appears as a thin, linear, slightly hyperdense, or markedly hypointense structure on CT and T2-weighted images, respectively (Fig. 2).[4]

Potential Postsurgical Complications

Infection

Postoperative infection of the affected eye is a rare, early complication of lens replacement with a reported risk of endophthalmitis of 0.01%-0.1%.[5] Early infections can be successfully managed with antibiotics alone. Advanced infections, which may involve the entire globe and/or adjacent orbital tissues consistent with endophthalmitis or

https://doi.org/10.1053/j.ro.2019.03.004
0037-198X/Published by Elsevier Inc.

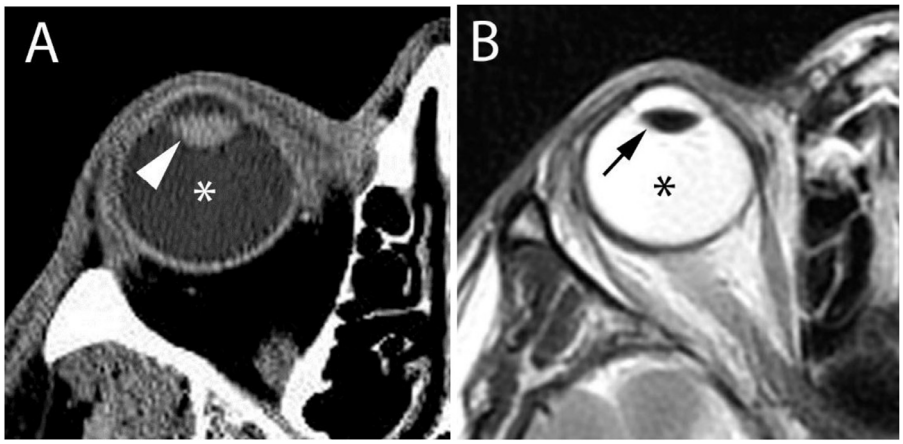

Figure 1 Axial CT (A) and T2-weighted (B) images illustrate the normal appearance of the biconvex native lens that is hyperdense (arrowhead) to vitreous body (*) on CT and hypointense (arrow) on T2-weighted images.

panophthalmitis, respectively, may require enucleation for a painful blind eye in some patients (Fig. 3). Retinal and scleral calcifications or frank phthisis bulbi may develop as sequelae of a severe infection if enucleation was not needed, usually leading to a functionally blind eye.

Ocular Hypotony

Ocular hypotony is another rare, early complication of intraocular lens replacement. In the postsurgical setting, this condition is thought to be caused by decreased intraocular pressure secondary to irritation and edema of the adjacent

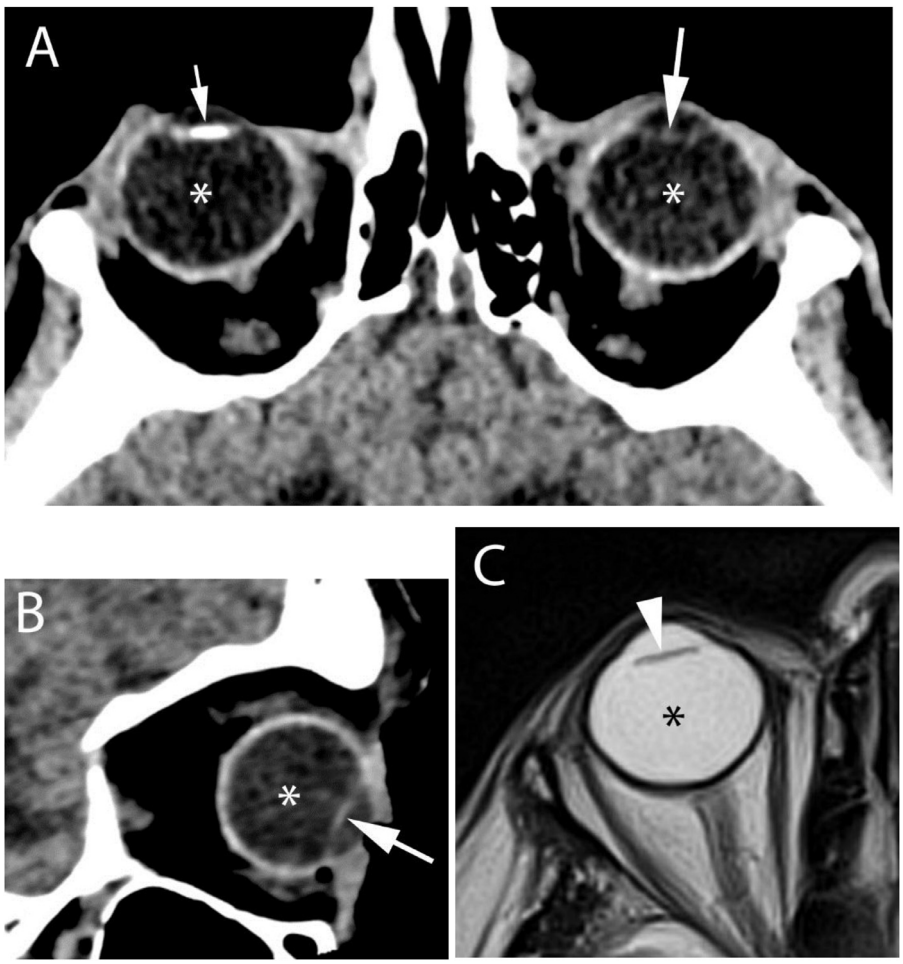

Figure 2 Axial (A) and sagittal CT (B) as well as T2-weighted (C) images demonstrate the normal appearance of a pseudophakic lens (arrows). Some prosthetic lenses are more dense on CT (small arrow in A) while others are more lucent (large arrow in A and B) when compared to the vitreous body (*). Both types are hypointense (arrowhead) to the vitreous body (*) on MRI.

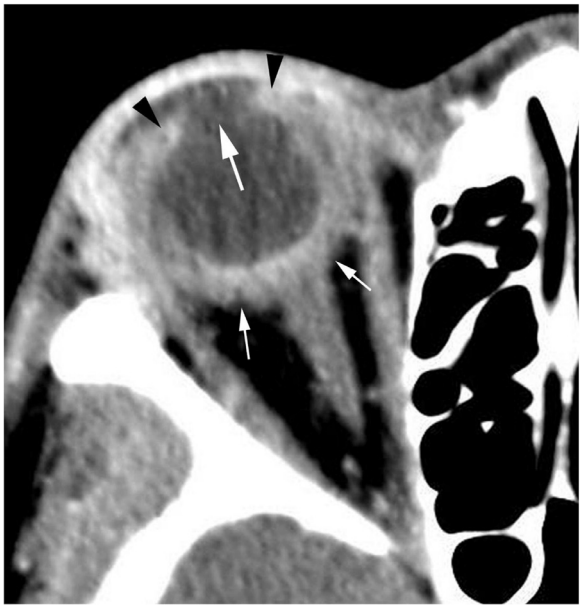

Figure 3 Axial CT image of a patient status post recent lens replacement shows lack of the native biconcave lens (large arrow) with associated marked thickening and enhancement of the sclera (small arrows) as well as of the iris (arrowheads) consistent with panendophthalmitis.

ciliary body.[6] On imaging, postoperative ocular hypotony manifests as globe deformity, intraocular gas accumulation and narrowing of the anterior chamber (Fig. 4).[7] It is critical to recognize ocular hypotony as it can lead to visual loss, chronic globe deformity, and phthisis bulbi if not treated timely. Its treatment is primarily medical and directed at reducing inflammation, but may require surgery to restore intraocular pressure.[6]

Lens dislocation

As with the native lens, a replaced intraocular lens may dislodge at any time in the postoperative phase with a reported risk of 1.2%. It may cause significant deterioration of vision.[8] The artificial lens might dislocate anteriorly or posteriorly and result in a narrowed or widened appearance of the anterior chamber, respectively. The dislocation can be complete, with the lens typically lying in the dependent portion of the vitreous body, or partial, where the artificial lens is still in part attached to the native lens capsule (Fig. 5). The partial dislodgement is often overlooked and might only be detected when scrolling through the axial data set and noticing uneven size of the anterior chamber from superior to inferior or with sagittal reformations along the long axis of the globe.

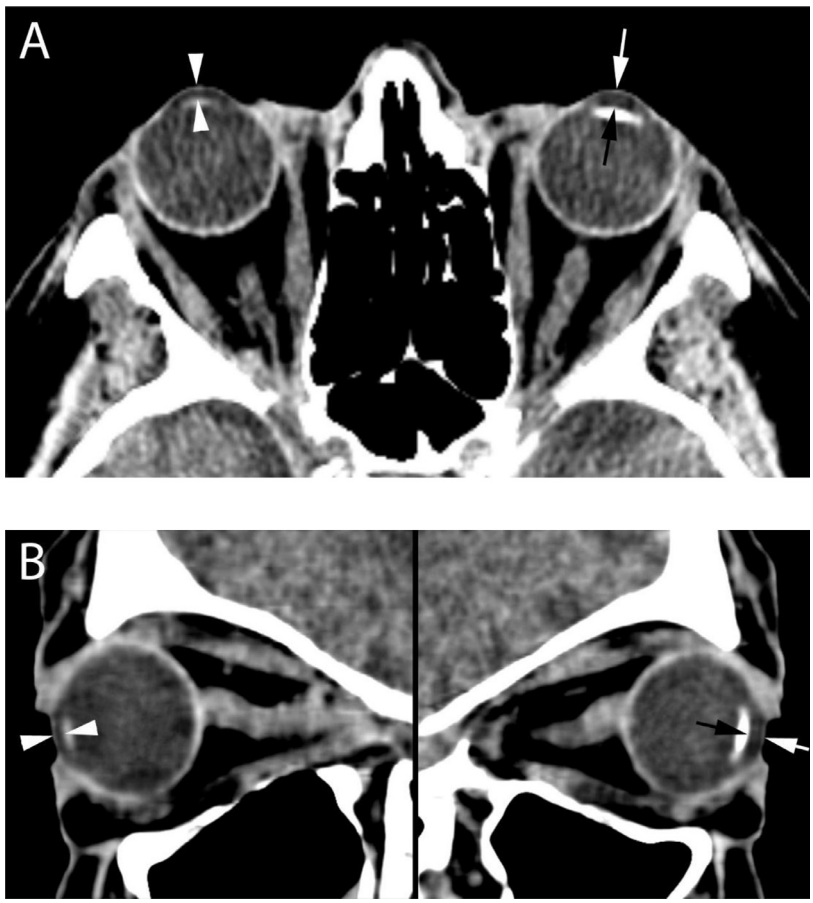

Figure 4 Axial (A) and sagittal (B) CT images of a patient status post bilateral lens replacements reveals a markedly narrowed anterior chamber on the right (between arrowheads) when compared to its normal appearance on the left (between arrows) consistent with ocular hypotony.

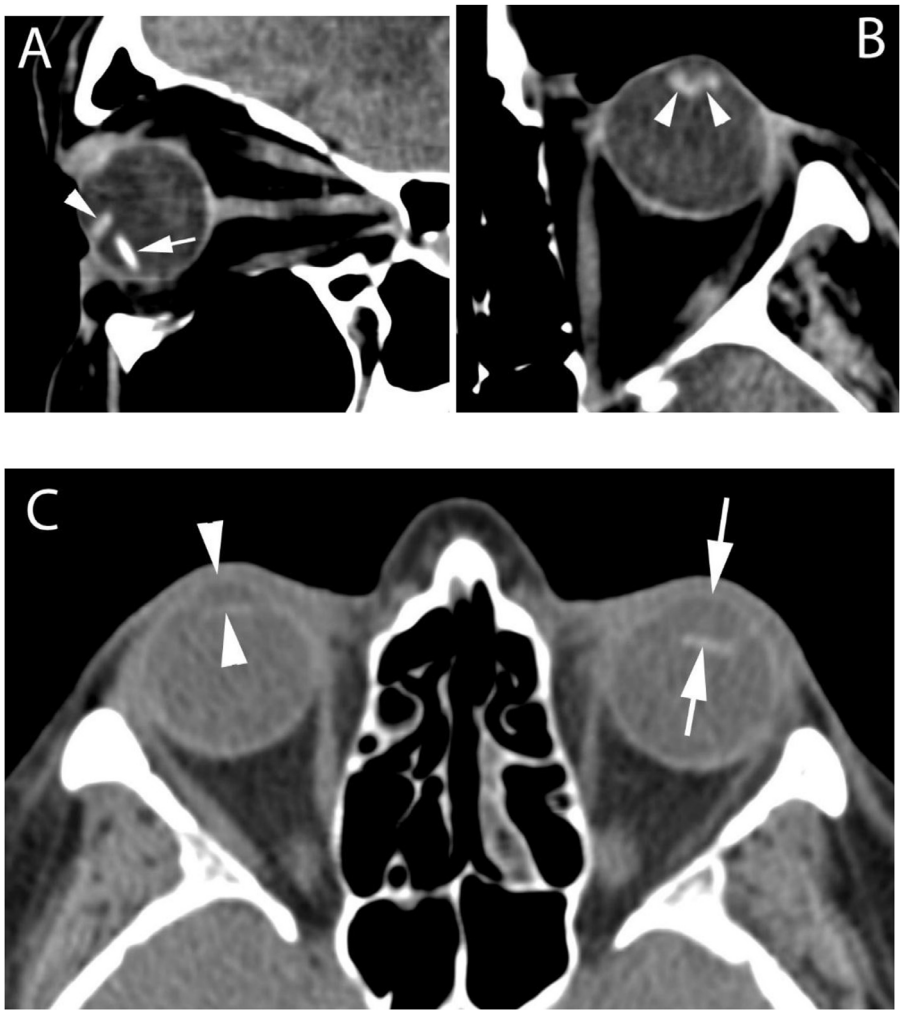

Figure 5 Sagittal CT image (A) demonstrates a markedly inferiorly and posteriorly displaced artificial lens (arrow in A) with associated posterior tilting of the iris (arrowhead in A). Artificial lens displacement is not always as obvious on imaging and might be associated with a wavy appearance of the iris (arrowheads in B) or present with enlargement of the anterior chamber (between arrows in C) when compared to the normal right side (between arrowheads in C). Such an enlargement of the anterior chamber may also be caused by postoperative glaucoma development.

Capsular Opacification

Postsurgical capsular opacification is thought to be due to proliferation and abnormal differentiation of migrated residual lens epithelium around the native residual capsule. It can be classified into an anterior and posterior type with the latter occurring in up to 50% of patients.[9] The posterior capsular opacification can be devided into fibrous and pearl types and is often located at the fusion of the anterior and posterior capsules, manifesting as hypointense nodularity along the posterior lateral or medial edge of the artificial lens on the T2-weighted images with variable degree of enhancement (Fig. 6).

Glaucoma

Glaucoma is a late complication of cataract surgery and thought to be caused by mechanical irritation of the iris by the artificial lens and subsequent uveitis.[5] This complication may be incidentally detected as an enlarged anterior chamber on routine cross-sectional imaging studies even years after lens replacement (Fig. 5C). Although rare, raising suspicion for the development of glaucoma is critical to avoid irreversible vision loss. Treatment is directed at reducing intraocular pressure either medically or surgically with a peripheral laser iridotomy or glaucoma shunt placement.[10]

Mimics of Complications

Anterior dislocation of the artificial lens leads to narrowing of the anterior chamber and might mimic ocular hypotony (Fig. 4). Ocular hypotony, however, typically occurs in the early postoperative phase and therefore is usually associated with the presence of a small amount of air within the globe.

Glaucoma Drainage Devices

Aqueous humor is produced by the ciliary body and flows from the posterior to the anterior chamber to subsequently

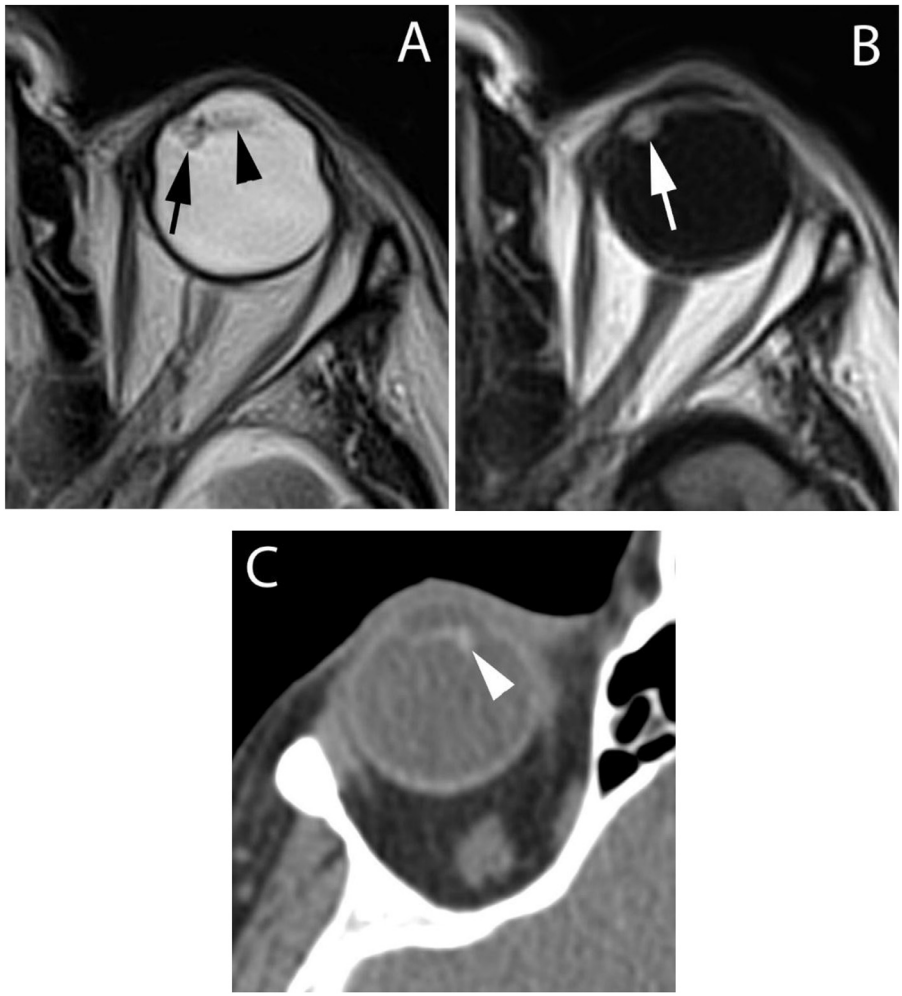

Figure 6 Axial T2-weighted image (A) reveals nodular irregularity (arrow in A) along the posterior aspect of the medial iris in a patient status post pseudophakic lens placement (arrowhead) which shows marked enhancement (arrow in B) on the axial gadolinium enhanced T1-weighted image (B) consistent with nodular posterior capsular opacification or fibrosis. This can be sometimes also observed on CT (C) with more linear opacification (arrowhead in C) along the posterior medial iris in a different patient.

drain via the trabecular meshwork into the canal of Schlemm. In glaucoma patients, there is either decreased drainage from the posterior to the anterior chamber (primary angle closure glaucoma) or reduced drainage into the canal of Schlemm (primary open angle glaucoma). Both of these mechanisms produce ocular hypertension, which eventually causes retinal ganglion cell death and irreversible visual field deficits.[11]

Initially, glaucoma patients are treated medically or with surgical opening into the trabecular meshwork or through the iris via peripheral iridotomy, depending on the glaucoma type. Disease progression is common and may necessitate placement of a glaucoma drainage device.[11] There are several types of implantable glaucoma drainage devices, but they have a similar design that employs a tube to shunt aqueous humor from the anterior chamber of the globe into an end plate.[12] The end plate can be implanted in any quadrant of the orbit. Over time, a fibrous capsule develops around the end plate within which shunted fluid may accumulate to form a bleb.

There are 2 major types of glaucoma drainage devices in use: valved (eg, Ahmed and Krupin) and nonvalved (eg, Baerveldt and Molteno). The purpose of the valve is to prevent excessive shunting of aqueous humor in the early postoperative period, which can lead to ocular hypotony. Over a period of weeks to months, the fibrous capsule surrounding the end plate serves as an osmotic barrier and reduces shunting by the nonvalved glaucoma drainage devices, thereby minimizing the risk of ocular hypotension.[12] Materials used for glaucoma pump manufacturing include silastic tubing and either silicone or polypropylene for the end plate which are naturally nonradiopaque. The Baerveldt end plate is, however, impregnated with barium. In addition, there is an intraocular glaucoma shunt (eg, Ex-PRESS shunt) in use consisting of a 2-3 mm stainless steel device that is inserted underneath a scleral flap at the limbus to shunt aqueous humor directly from the anterior chamber into an episcleral fluid bleb.[4] Some patients might have multiple different glaucoma shunts in place in one eye.

Normal Imaging Appearance

The endplates of many of the currently used glaucoma drainage devices are easily visualized on CT due to inherent hyperdensity of some or all parts of the device, with the nonvalved Baerveldt shunt being most radiopaque due to barium impregnation (Figs. 7 and 8). Only the nonvalved Molteno and the Krupin shunts are difficult to appreciate on CT, as these are predominantly radiolucent and show similar CT density as the intraorbital fat.[4] The end plates are difficult to visualize on all MRI sequences due to small size and very low attenuation (Fig. 9). On MRI, the presence of a glaucoma drainage device is usually best noticed through visualization of the coincidental fluid filled bleb adjacent to the end plate. Such a bleb develops in the early postoperative period and represents an expected finding when exhibiting signal intensity of simple fluid on all sequences without adjacent inflammatory changes (Fig. 10).[4] The intraocular Ex-PRESS shunt is visible on CT as a punctate radiopaque foreign body in the anterior chamber, most commonly in its superior aspect (Fig. 11). The small size of the Ex-PRESS shunt makes it a challenge to visualize on MRI. It can be only identified as a dark round structure when a volumetric acquisition with high spatial in-plane resolution is used.[4]

Potential Postsurgical Complications

Ocular Hypotony

Ocular hypotony is a common complication of nonvalved glaucoma shunts in the first few weeks to months following surgery as it takes time to develop a mature encapsulation around the end plate. It primarily manifests on imaging as flattening of the anterior chamber without or with coexistent choroidal effusion. Choroidal effusion occurs in 13%-16% of patients and is thought to be caused by an elevated pressure gradient across the capillary bed in the setting of declining intraocular pressure.[13] CT and MR depict choroidal effusion as an irregular contour of the inner surface of the globe with discrete suprachoroidal collections of fluid (Fig. 12). Associated clinical symptoms vary from being asymptomatic to having marked visual impairment that may require medical or surgical treatment.

Infection

Endophthalmitis following a glaucoma shunt surgery occurs in about 2% of patients. Onset is usually delayed to about 6 weeks after surgery, due to the shunt tubing causing erosion of the conjunctiva, becoming exposed and providing a pathway for bacteria to enter the globe.[14] Most cases of endophthalmitis can be managed medically in combination with surgical repair of the globe erosion. However, some cases progress to panophthalmitis and may require removal of the implant or entire globe.

In the early postoperative phase, dacryoadenitis may occur as the majority of the glaucoma drainage devices are placed in the upper outer quadrant of the orbit. Occasionally, a localized abscess is formed that might be difficult to distinguish from a physiological bleb that is associated with a glaucoma shunt (Fig. 13).

Mimics of Complications

Several weeks after implantation of a glaucoma drainage device, it is normal to have a fluid bleb adjacent to the end plate. This bleb should not be mistaken for an abscess. This is most problematic on MRI since the glaucoma shunt end plate can be challenging to visualize. The lack of adjacent inflammatory changes should lead to the correct diagnosis. The radiologist has to be careful not to mistake the physiological enhancement of the adjacent lacrimal gland as peripheral enhancement of the bleb.

The Ex-PRESS shunt might be mistaken for a radiopaque foreign body, if the radiologist is not aware of its normal imaging appearance and its typical position in the superior aspect of the anterior chamber (Fig. 11A).[4]

Retinal Detachment Surgery

Retinal detachments occur in 5-10 per 100,000 people annually. The rhegmatogenous type is most common and is caused by a retinal tear that leads to accumulation of fluid in the potential subretinal space between the sensory retina and retinal pigmented epithelium. Early surgical intervention, with the goal to close the retinal tear and reapproximate the 2 retinal layers, is critical to preserve vision. There are several methods available to the ophthalmologist to accomplish this, with many patients undergoing multiple surgical types of interventions simultaneously or over time.

A small retinal tear can be closed with retinopexy using cryotherapy, diathermy, or laser photocoagulation technology. For more advanced cases, a vitrectomy may be necessary with surgical removal of the gel like vitreous humor to provide better access to the retinal tear and to reduce the pulling forces of the vitreous upon the retina.[4] Vitrectomy is typically combined with globe insufflation with silicone oil or resorbable gas (also referred to as pneumatic retinopexy) to promote approximation of the retinal layers. The pneumatic retinopexy can be performed without vitrectomy as a minimally invasive procedure in an outpatient setting, by insufflation of room air lasting up to 1 week within the eye or using a long- acting gas (eg, sulfur hexafluoride, perfluoroethane, and perfluoropropane) that can last to up to 8 weeks.[15]

A common adjunctive treatment is surgical placement of a scleral band or buckle leading to external indentation of the globe. This reduces tension on the retina at the site of a retinal tear, allowing reapproximation of the sensory retina with the retinal pigmented epithelium.[4] The scleral band usually encircles the globe. A separate buckle may be applied orthogonally to the scleral band to allow for additional focal indentation if needed. Currently, silicon is the preferred material due to its durability. It can be applied in solid and sponge form. Hydrogel bands and buckles were used until the 1990s but became obsolete because of progressive swelling

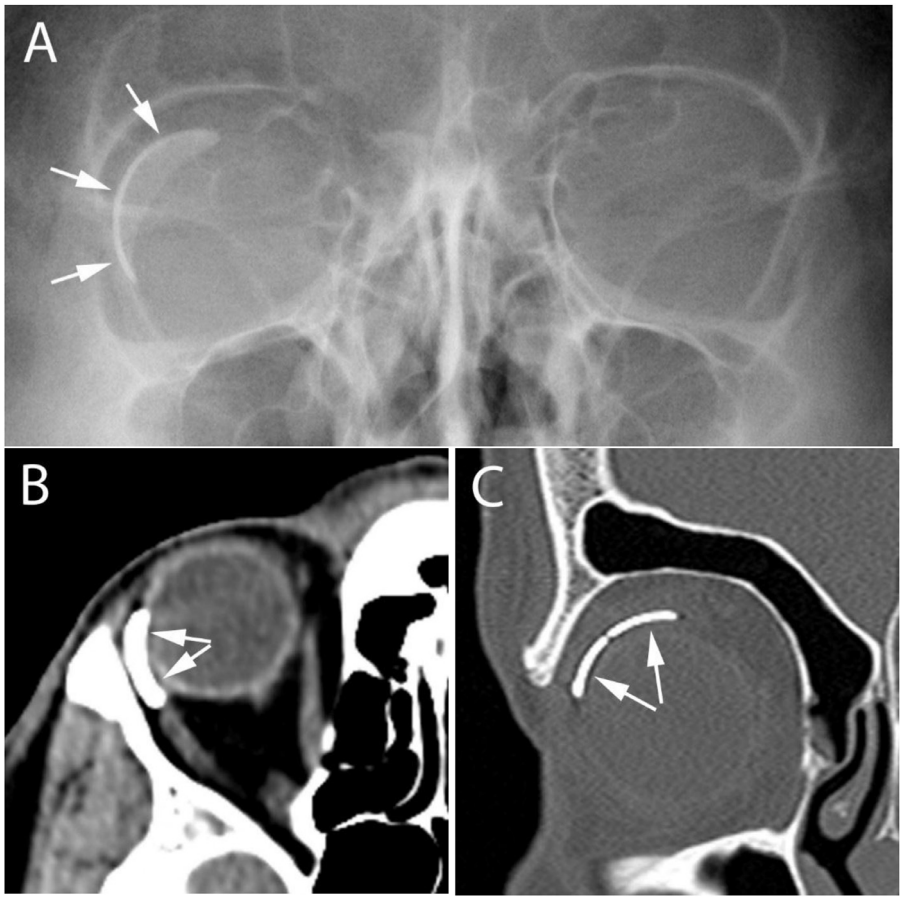

Figure 7 Plain film of the orbit obtained in anterior posterior direction (A) as well as CT images in axial plane displayed in soft tissue window (B) and in coronal plane in bone window (C) show a curvilinear density in the right orbit (arrows). This is the typical plain film and CT appearance of the barium impregnated, nonvalved Baerveldt shunt. It is most commonly placed in the upper, outer quadrant of the orbit as in this patient.

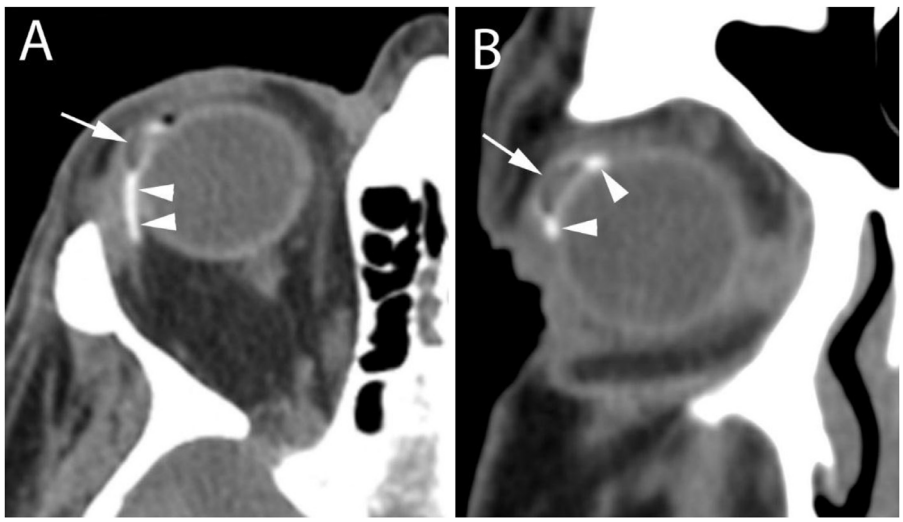

Figure 8 Axial (A) and coronal (B) CT images reveal the normal appearance of the valved Ahmed glaucoma shunt. It consists of a radiolucent reservoir (arrow) and slightly hyperdense curvilinear parts of the endplate (arrowheads in A) that are more punctate in appearance in the coronal plane (arrowheads in B). Ahmed shunt is not visible on plain films (not shown).

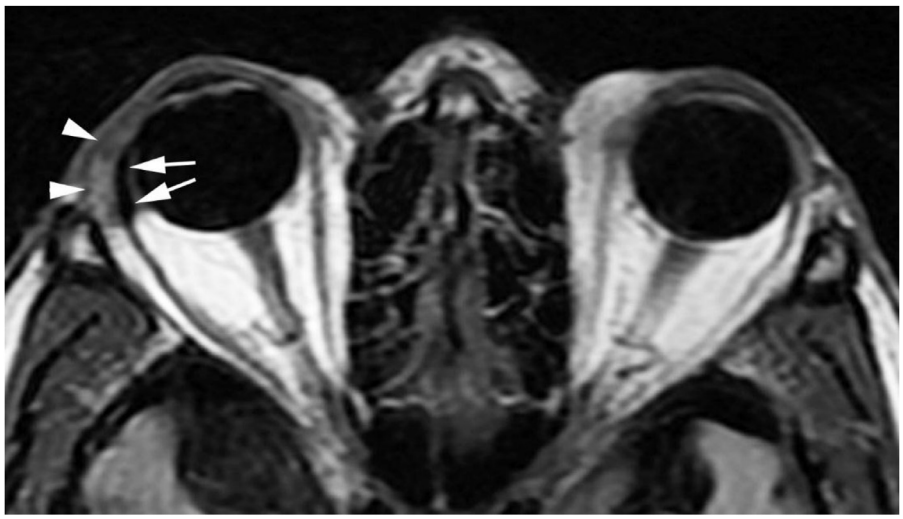

Figure 9 Axial T1-weighted image through the orbit reveals subtle curvilinear hypointensity in the right lateral orbit (arrows) with mild adjacent obliteration of the extraconal fat planes (arrowheads) consistent with nonvalved glaucoma shunt. These subtle changes are more apparent when comparison to the normal left orbit is made.

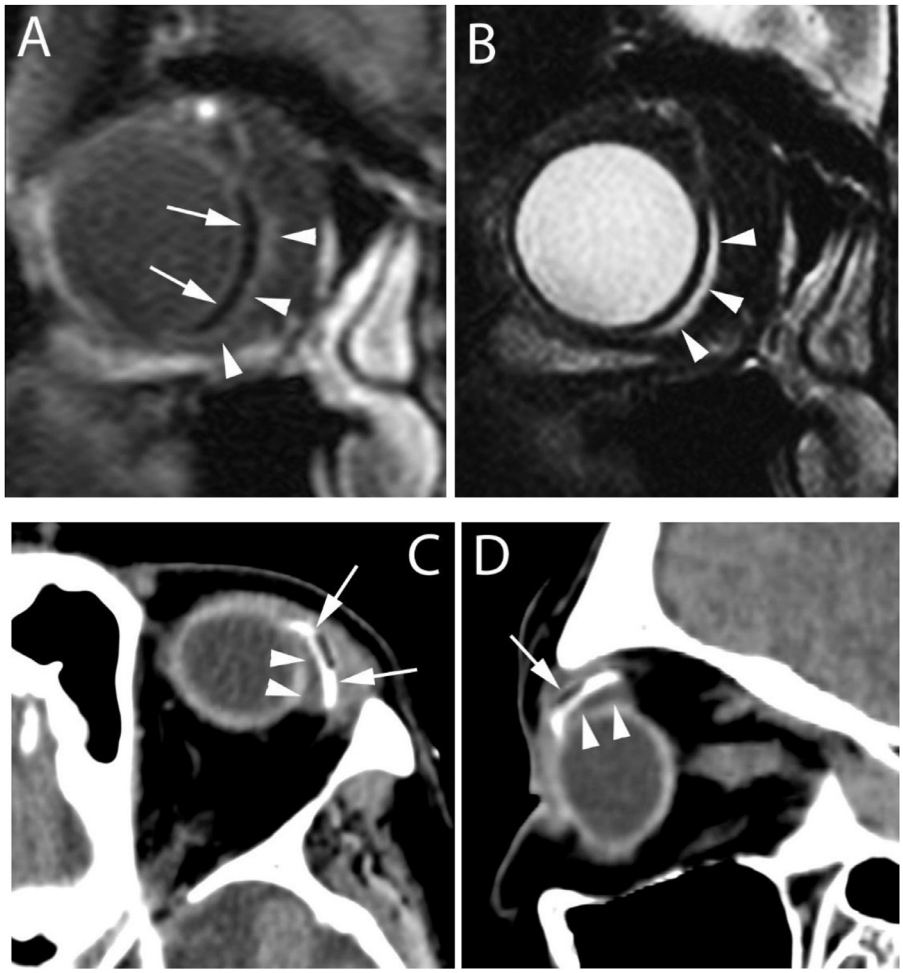

Figure 10 Coronal, gadolinium enhanced, fat suppressed T1-weighted image (A) demonstrates a crescentic low attenuation structure along the inferior medial globe (arrows) with minor adjacent enhancement (arrowheads in A) that is associated with a crescentic fluid collection (arrowheads in B) on the fat suppressed, coronal T2-weighted image (B) without adjacent inflammatory changes. These imaging findings are consistent with the normal appearance of a nonvalved glaucoma shunt that is associated with a small bleb. Such bleb (arrowheads in C and D) can also be seen on CT as illustrated in axial (C) and sagittal (D) planes in a different patient with a valved glaucoma shunt (arrows in C and D).

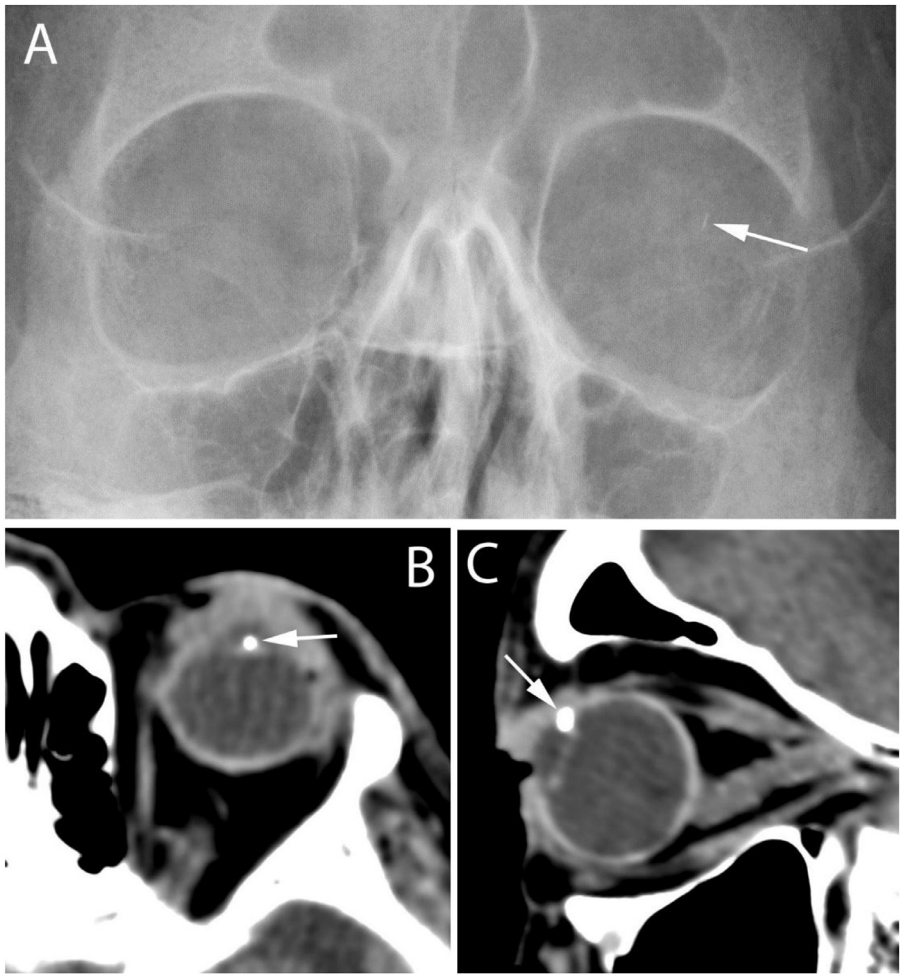

Figure 11 Plain film of the orbit obtained in anterior posterior direction (A) shows a 2-3 mm linear, radiopaque foreign body (arrow in A) in projection over the left superior orbit. The axial (B) and sagittal (C) CT images reveal a punctate density in the superior aspect of the anterior chamber (arrows in B and C). This is the typical plain film and CT appearance and location of an intraocular glaucoma shunt.

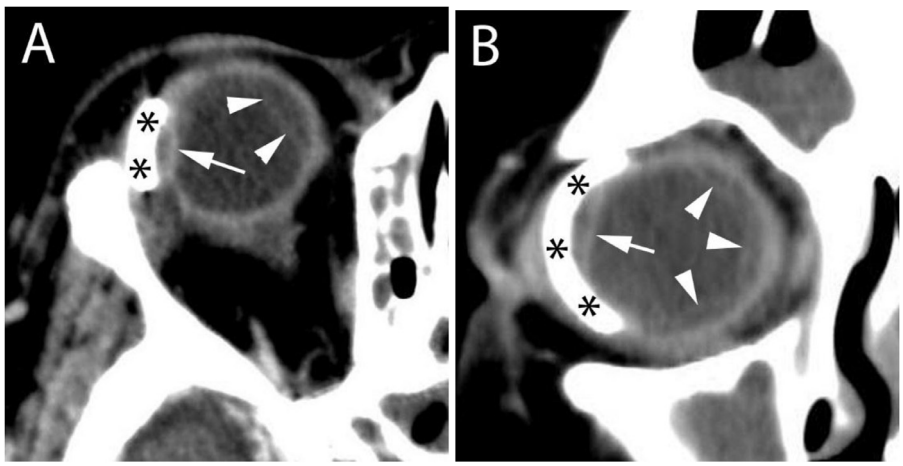

Figure 12 Axial (A) and coronal (B) CT images show a small fluid collection (arrow) medial to the nonvalved glaucoma shunt (**) that causes deformity of the lateral globe. Such mass effect upon the globe is not consistent with a physiological bleb related to adjacent glaucoma shunt. Careful evaluation of the rest of the globe reveals additional areas of separation of the layers of globe (arrowheads) that are aligned parallel to each other in the axial plane consistent with a choroidal effusion.

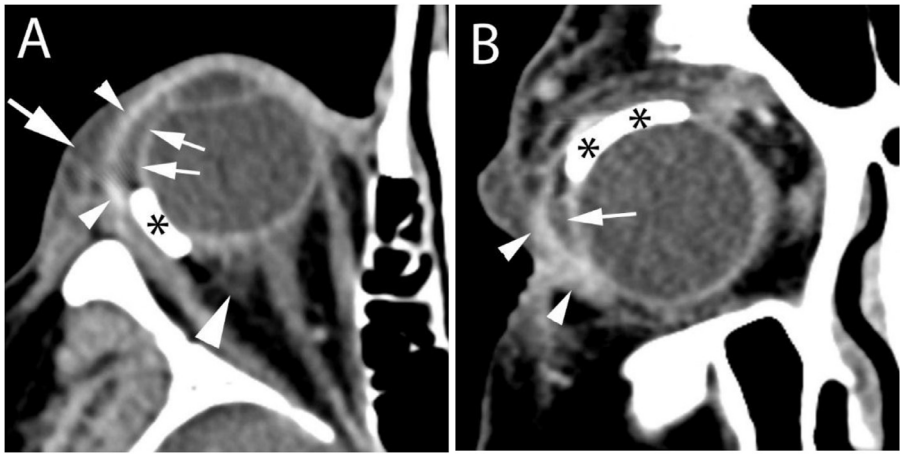

Figure 13 Axial (A) and coronal (B), contrast enhanced CT images in a patient status post recent nonvalved glaucoma shunt placement demonstrate a small fluid collection (small arrows) that is anterior and inferior to the glaucoma shunt (*) rather than in the physiologically expected location adjacent to the shunt. This is concerning for abscess formation which is confirmed by the marked rim enhancement (small arrowheads in A and B), preseptal soft tissue swelling (large arrow in A) and intraconal fat stranding (large arrowhead in A).

and fragmentation of the hydrogel material years following surgery and requiring surgical removal.[16]

Normal Imaging Appearance

The postsurgical changes from vitrectomy and retinopexy are not directly visible on imaging. Only the effects of the globe insufflation procedure when performed as part of the retinal detachment repair can be detected. Silicone oil has high attenuation on CT while it is hypointense to fluid on T2 and slightly hyperintense on T1-weighted images (Fig. 14).[4] In addition, a crescent shaped chemical shift artifact is usually noticed on conventional MR sequences owing to the distinct resonant frequency of protons in silicone oil compared to water (Fig. 14).[4] Resorbable gas has properties of air on imaging, and as such is markedly hypoattenuating on CT and is devoid of signal on all MR sequences. This is often seen with a small fluid level in the dependent portion of the globe (Fig. 15).[4]

Scleral band or buckle devices have a variable appearance on CT, with solid silicone being hyperdense and silicone sponge material assuming air attenuation (Figs. 16 and 17).[4] On MRI, solid silicone and silicone sponge are both hypointense on T1-weighted and T2-weighted sequences and may be difficult to visualize if small in size (Figs. 16D and 17B). Indentation of the globe by a scleral band or buckle device is expected and might be the only sign of such a procedure on MRI (Fig. 18).

Potential Postsurgical Complications

Scleral Buckle/Band Dislodgement

A scleral buckle/band may dislodge over time and cause scleral invasion. This can be easily detected when postsurgical baseline imaging is available for direct comparison. Expected indentation of the globe is usually smooth in case of a buckle and circumferential in case of a band (Fig. 18). On the contrary, an abrupt, focal contour deformity should raise the suspicion for scleral invasion with scleral band/buckle dislodgement (Fig. 19).

Infection

Postoperative infection is a rare complication of retinal detachment repair with reported risk of up to 2%.[17] An endophthalmitis might be challenging to detect in such patients as the superficial tissues and the globe have been manipulated during the procedure. Therefore, presence of retrobulbar inflammatory changes might be the best but an unfortunately late imaging indicator of postsurgical infection.

Mimics of Complications

Intraocular silicone oil can be mistaken for vitreous hemorrhage on CT and MRI. On CT, the silicon oil experiences high but homogenous density. On the contrary, vitreous hemorrhage is usually heterogeneous in distribution and might show a hematocrit level or a gradient in density, with highest density in the dependent portion of the globe.[18,19] On MRI, the presence and orientation of the chemical shift artifact along the frequency encoding direction provide important clues to the correct diagnosis.[20]

The injected resorbable gas in the globe may be mistaken for a penetrating injury in the setting of acute trauma. Lack of edema and/or hematoma in the preseptal soft tissues corresponding to a trajectory track as well as preservation of the shape of the globe usually help to establish the diagnosis.[19]

Scleral buckles made from silicone sponge or hydrogel are radiolucent and can mimic a foreign body in the setting of trauma, namely a retained wooden foreign body (Fig. 20).[19]

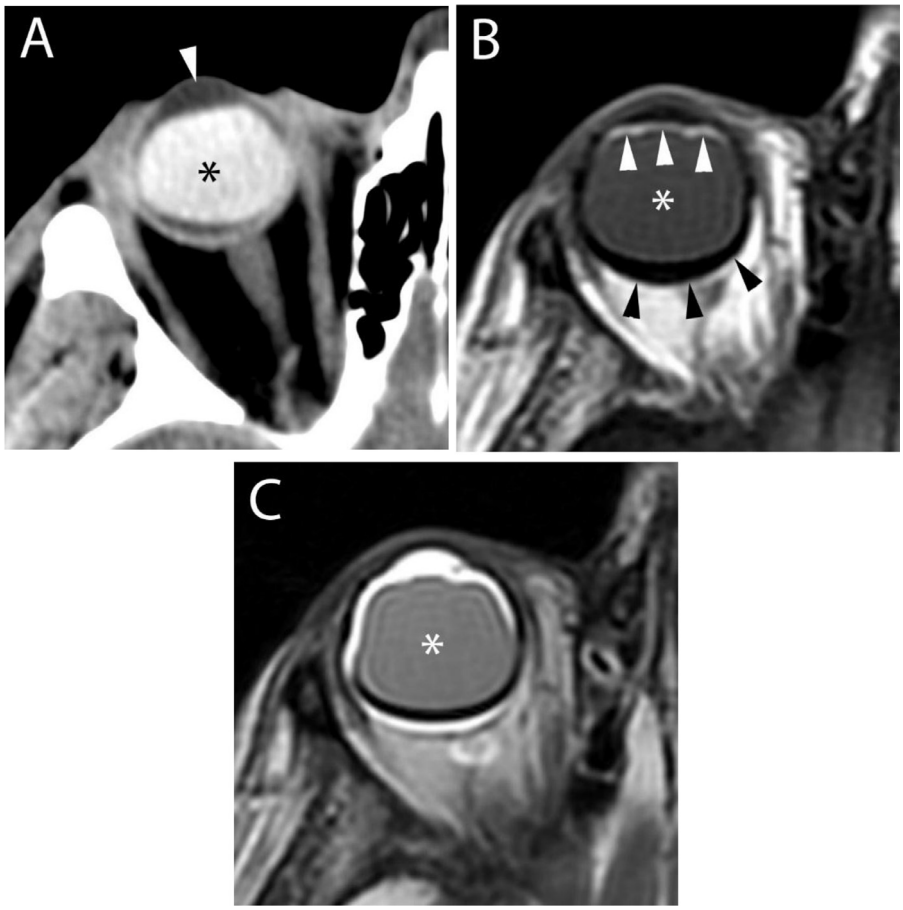

Figure 14 Axial CT image (A) shows a homogenously hyperdense vitreous body (*) in comparison to the normal fluid attenuation of the anterior chamber (arrowhead). This is consistent with vitrectomy and subsequent intraocular silicone injection. On MRI, the silicon assumes a slightly hyperintense appearance (*) on the T1-weighted (B) image and hypointense attenuation (*) on T2-weighted (C) sequence when compared to fluid. This is combined with a hyperintense artifact along the anterior edge of the silicone (white arrowheads) and a dark, crescentic rind (black arrowheads) along the posterior edge of the silicone on the T1-weighted images that is related to a chemical shift artifact.

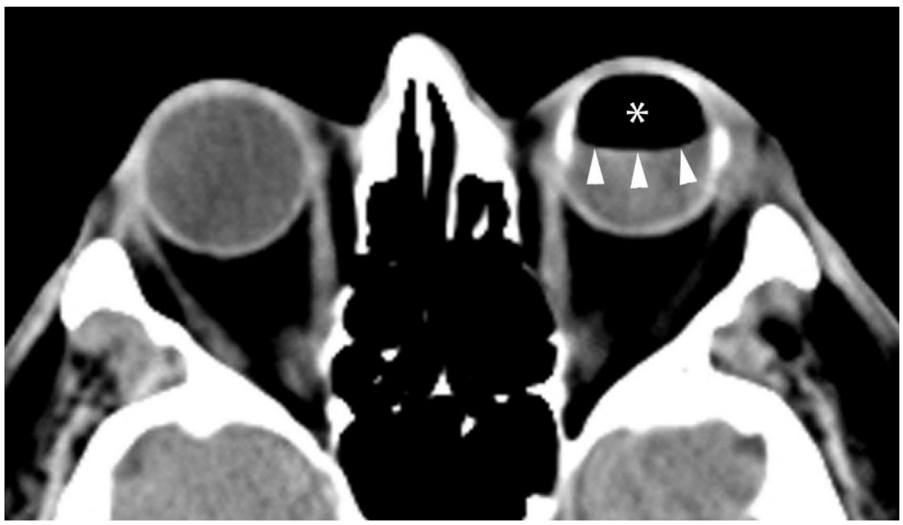

Figure 15 Axial CT image illustrates the normal appearance of the globe following insufflation of gas (*) into the left globe to facilitate apposition of the retina to the sclera. This is referred to as pneumatic retinopexy and usually shows an air fluid level (arrowheads) as it this patient.

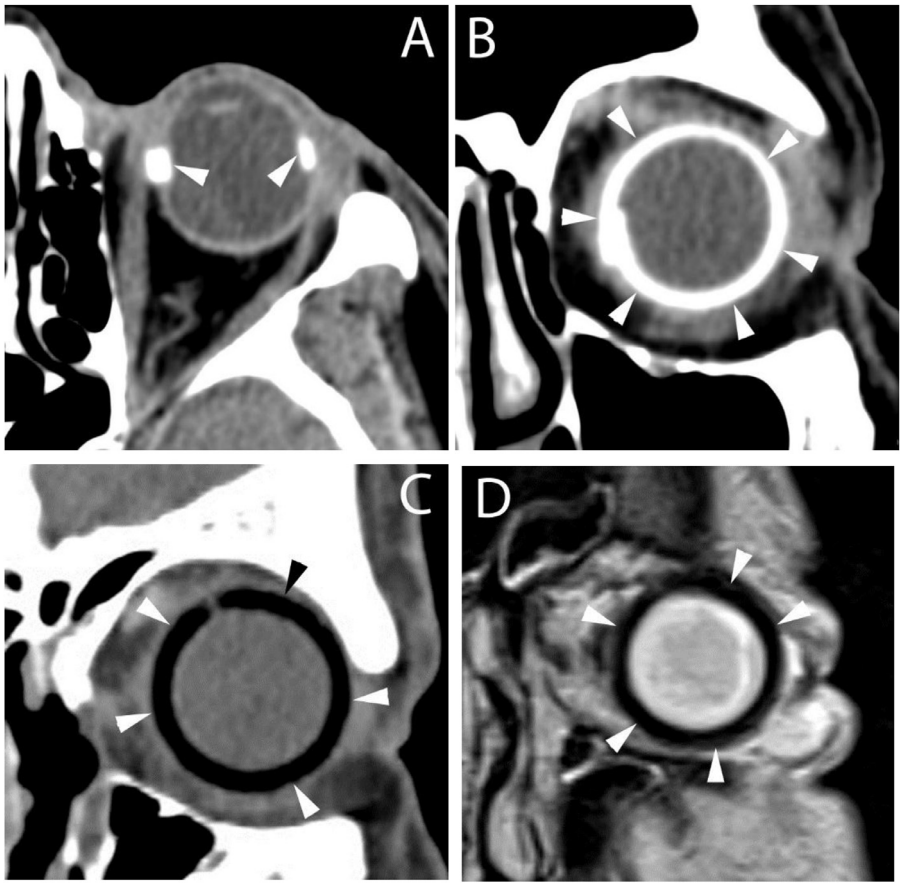

Figure 16 Axial (A) and coronal (B) CT images illustrate the normal appearance of a solid silicone band that is hyperdense (arrowheads in A) when compared to the adjacent globe and is circumferential in nature (arrowheads in B). In contrast, silicone sponge and hydrogel materials are very hypodense (arrowheads in C) on CT similar to air. On MRI, these 2 materials are indistinguishable from each other and assume hypointense signal (arrowheads in D) on all sequences as demonstrated here on a T2-weighted sequence (D).

Lack of edema and/or hematoma in the preseptal soft tissues along the trajectory track as well as a coexisting scleral band should lead to the correct diagnosis as scleral buckles are often placed in combination with scleral bands. MRI, in particular STIR or fat-suppressed T2-weighted images, are also more sensitive in detection of inflammatory changes around a foreign body that are not observed with silicone sponge material after the immediate postoperative phase.[19]

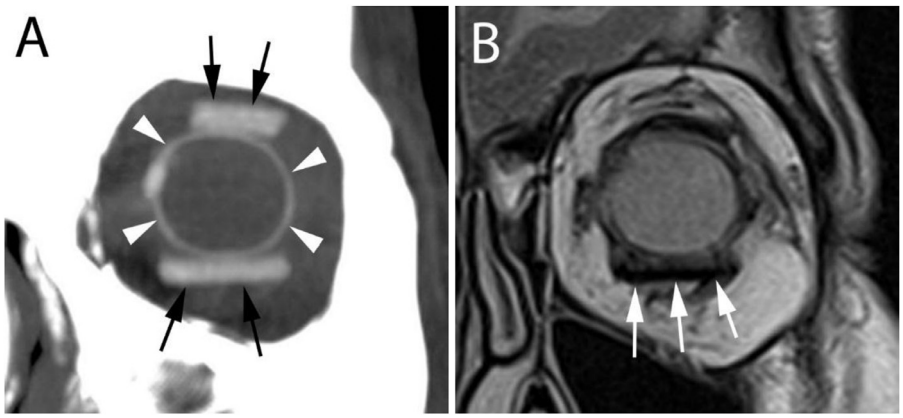

Figure 17 Coronal maximum intensity image (A) shows a scleral silicone band (arrowheads) around the globe (*) as well as silicone buckles (arrows in A) superior and inferior to the globe. The scleral buckles are of very low attenuation on the MRI and therefore difficult to appreciate as illustrated on this coronal T2-weighted image (B) on which the inferior scleral buckle (arrows in B) is clearly seen while the superior one and the silicon band are not appreciable.

Figure 18 Axial T2-weighted image demonstrates changes of scleral banding bilaterally. On the right, the deformity of the globe is minor (arrowhead) and difficult to appreciate while on the left side there is marked indentation (between arrows) of the left mid globe. This might be necessary to be able to adjoin the retina to the sclera.

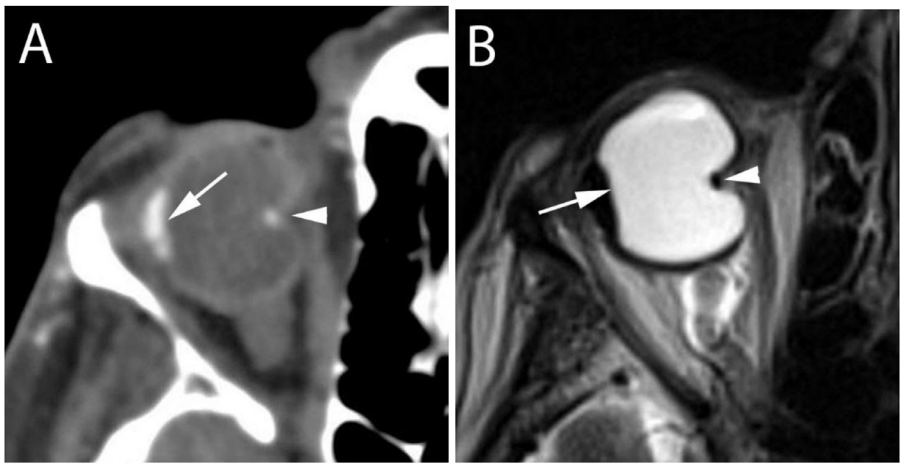

Figure 19 Axial CT (A) and T2-weighted (B) images demonstrate abrupt indentation (arrowhead) of the medial globe in contrast to the mild indentation (arrow) upon the lateral globe. This is rather atypical for scleral banding and should raise the suspicion for scleral band dislodgement.

Ocular Prostheses

Surgical removal of the globe is termed enucleation. In order to achieve a satisfactory cosmetic outcome after an enucleation an ocular prosthesis is placed. The prosthesis usually consists of 2 components: an anterior shell and a posterior sphere. The anterior shell is usually removable and either made out of glass or acrylic resin. It is decorated with a custom design to match the contralateral eye as best as possible to provide the most optimal cosmetic result.[4] The posterior sphere is nonremovable and is either porous or nonporous. Currently, the porous subtype is preferred as it facilitates fibrovascular ingrowth with superior motility and less postoperative complications particularly implant extrusion. The porous spheres can be made of synthetic hydroxyapatite, aluminum oxide, or polyethylene.[4] Nonporous ocular implants are still in use and can be made out of silicone, methylmethacrylate, metal, or glass.

In addition to cosmetic consideration, motility simulating conjugate eye movements is a desirable quality after ocular prosthesis placement. Therefore, the extraocular muscles are typically attached to the sphere to provide coordinated movement between the 2 eyes.[4]

Normal Imaging Appearance

The anterior shell is crescentic in shape and located immediately underneath the eyelid. It might be separated from the sphere by small amount of air (Fig. 21A). The posterior sphere can assume variable attenuation depending on the

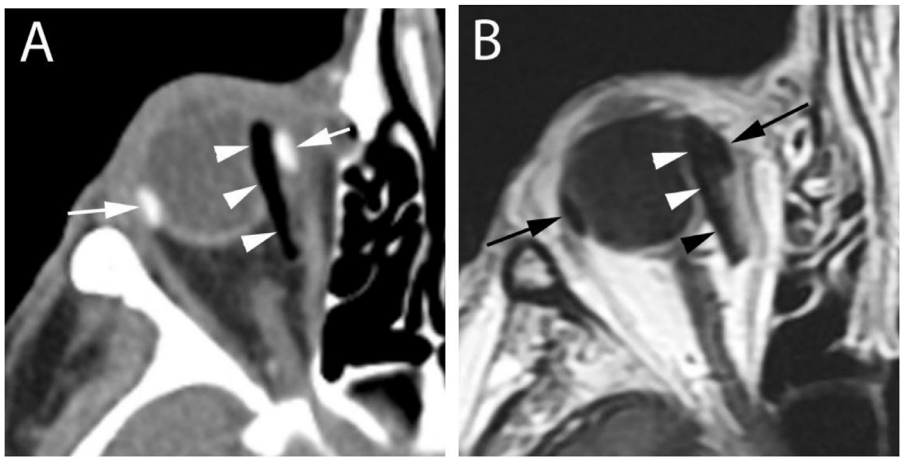

Figure 20 Axial CT (A) and T1-weighted (B) images reveal a low attenuation linear structure (arrowheads) along the medial orbit. This could be mistaken for a nonradiopaque foreign body such as wood. The association with a scleral band (arrows) should raise the suspicion that this represents a hydrogel or silicone sponge buckle that is often used in combination with a scleral band for treatment of retinal detachment. In addition, the lack of preseptal edema should lead to the correct diagnosis.

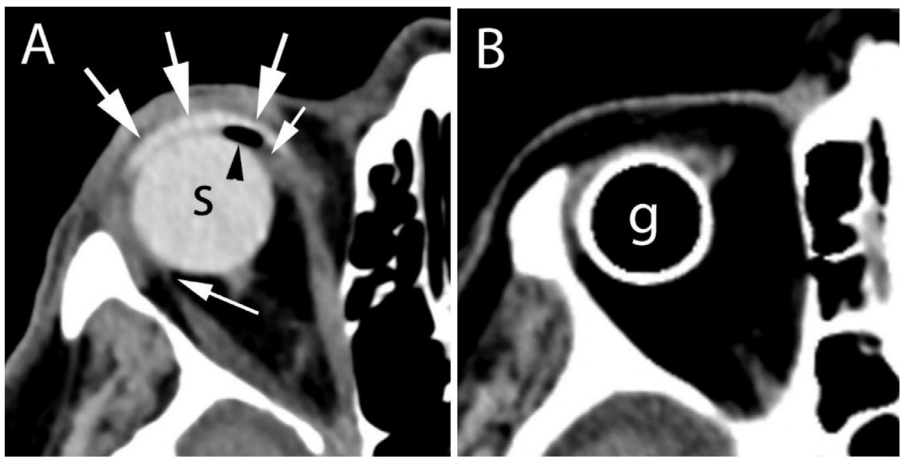

Figure 21 Axial CT image (A) reveals an ocular prosthesis with an anterior shell (large arrows) and a silicone sphere (s) with small amount of air between the 2 (arrowhead). Notice that the extraocular muscles are attached to the sphere (small arrows) facilitating coordinated movement with the left eye. Axial CT image (B) of a different patient, shows a glass sphere with a hollow center (g) without an anterior shell in place. Notice that none of the extraocular muscles are attaching to the glass sphere.

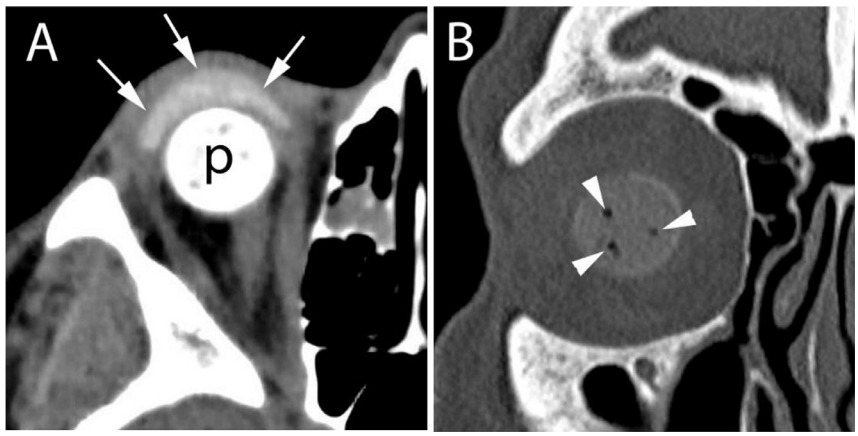

Figure 22 Axial CT image displayed in soft tissue window (A) demonstrates the normal appearance of a porous sphere (p) with an anterior shell (arrows) in place. The coronal CT image displayed in bone window (B) reveals small air pockets (arrowheads) within the porous sphere that is a normal finding in the first few weeks after ocular prosthesis placement. The size of the air pockets together with lack of fatty stranding around the prosthesis should lead to the correct diagnosis of a noninfected porous prosthesis—see also Figure 24.

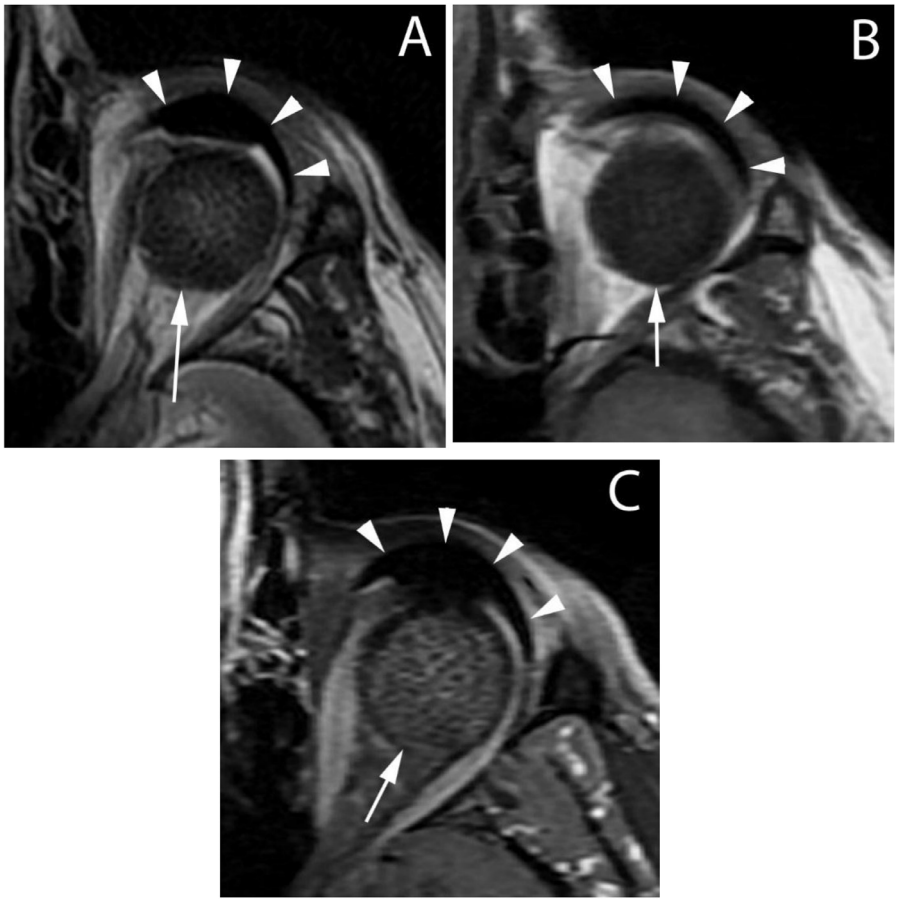

Figure 23 Axial T2-weighted image (A) shows an ocular prosthesis with an anterior shell (arrowheads) and a porous sphere (arrow) in place. The porous sphere (arrow) has a speckled, slightly T2 hyperintense appearance. Axial T1-weighted image (B) shows a posterior sphere (arrow) that has the appearance of a normal globe. Only the anterior shell (arrowheads) indicates that the patient is status post ocular prosthesis placement. Speckled, heterogeneous enhancement (arrow) is seen on the fat-suppressed, gadolinium enhanced T1-weighted image (C) consistent with fibrovascular ingrowth that should not be mistaken for an infection of the prosthesis.

material it is made off. A silicone sphere is usually homogenously hyperdense on CT while a glass or metal sphere has a dense rim with a hollow center (Fig. 21).[4] Both exhibit dark signal on MRI. The appearance of a porous implant, in particular when made out of hydroxyapatite, is more complex and depends on extent of fibrovascular ingrowth, the degree of associated demineralization of the implant and bone formation. Consequently, the porous sphere can show variable density on CT and exhibit attenuation changes on follow-up imaging (Fig. 22). Porous implants are dark on T1 and slightly hyperintense on T2-weighted images. Over time, the T2 signal of the implant diminishes as fibrovascular ingrowth progresses. In addition, fibrovascular ingrowth results in progressive, typically centripetal, contrast enhancement on serial imaging (Fig. 23).[4,21]

Potential Postsurgical Complications

Ocular implant exposure is one of the most common postoperative complications with a reported incidence of up to 14%.[22] This is a clinical diagnosis and imaging is rarely required.

Infection

Postoperative implant infection is rare, occurring in 1% of patients.[22] The porous type implant is more vulnerable to infection as its irregular matrix may serve as a site for bacterial seeding before the fibrovascular ingrowth is completed, which may take up to 1 year.[22] Imaging findings of postsurgical infection include gas accumulation in the implant beyond the expected early postoperative period, pre- and/or postseptal inflammatory changes, exuberant enhancement of the implant, and development of a discrete abscess.

Enophthalmos

Postsurgical enophthalmos is most commonly seen in the setting of prior orbital trauma requiring orbital reconstruction in combination with ocular prosthesis placement. The enophthalmos might be related to the post-traumatic distortion of the orbit and/or progressive postoperative scarring manifesting clinically as facial asymmetry, disonjugated gaze and/or fixed eye. On imaging, posterior displacement of the globe relative to the contralateral side is observed that might be associated with obliteration of the postseptal fat planes due to scarring.

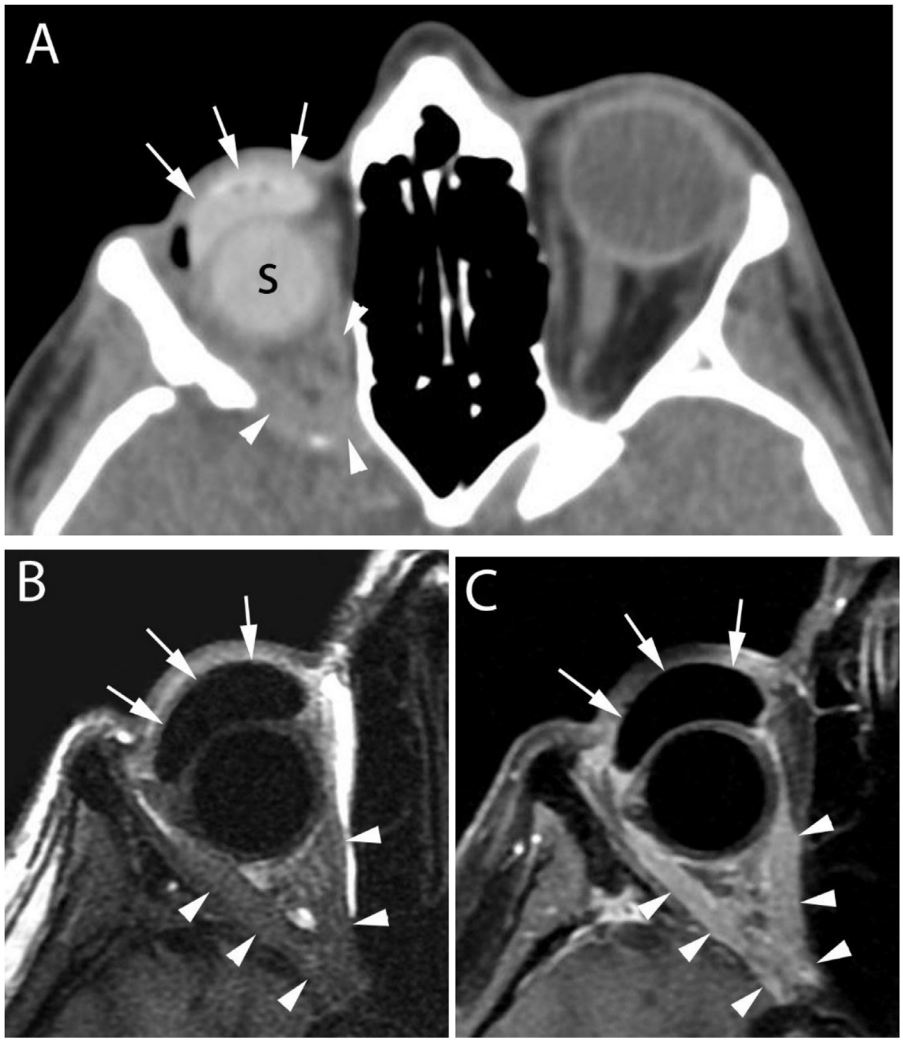

Figure 24 Axial CT image (A) demonstrates marked enophthalmos on the right when compared to the native left eye in a patient status post ocular prosthesis placement with an anterior shell (arrows) and a posterior silicone sphere (s) in place. Notice the loss of the retrobulbar fat (arrowheads) when compared to the left side that is confirmed on the T1-weighted image (B) corresponding to extraocular musculature. Marked, gadolinium enhancement (arrowheads) is noted in the extraocular muscles on the axial T1-weighted, gadolinium enhanced image (C) indicating acute to early subacute denervation of the extraocular muscles.

Mimics of Complications

The porous sphere tends to trap small pockets of *intrinsic* air in the early postoperative phase due to its porous structure. This should not be mistaken for implant infection. In addition, the porous implant shows progressive enhancement correlating with the fibrovascular ingrowth into the prosthesis material. Such progression of enhancement is expected within 1 year after surgery and should not be mistaken for an underlying infection. Lack of inflammatory changes or abscess around the implant usually confirms the correct diagnosis of expected postsurgical changes.

Denervation injury of the extraocular muscles is a rare occurrence. It manifests on imaging as edema and enhancement of the involved muscles in the acute phase (Fig. 24) and atrophy and fatty replacement in the chronic phase.

Conclusion

In an era of increasing surgeries for cataracts, glaucoma, retinal detachment, and various orbital reconstructions, the radiologist is faced with a variety of orbital implants and devices on a daily basis as the majority of head, neck, and maxillofacial imaging includes the orbits in the scanned volume. Therefore, the radiologist must be familiar with the expected postsurgical imaging appearance of the orbit to avoid false positive diagnoses and to facilitate detection of postoperative complications.

References

1. Gollogly HE, Hodge DO, St Suaver JL, et al: Increasing incidence of cataract surgery: Population-based study. J Cataract Refract Surg 39:1383-1389, 2013

2. Ramulu PY, Corcoran KJ, Corcoran SL, et al: Utilization of various glaucoma surgeries and procedures in Medicare beneficiaries from 1995-2004. Ophthalmology 114:2265-2270, 2007
3. Argal S: Newer inatraocular lens materials and design. J Clin Ophthalmol Res 1:113-117, 2013
4. Reiter MJ, Schwope RB, Kini JA, et al: Postoperative imaging of the orbital contents. RadioGraphics 35:221-234, 2015
5. Carlson AN, Steward WC, Tso PC: Intraocular lens complications requiring removal or exchange. Surv Ophthalmol 42:417-440, 1998
6. de Smet MD, Gunning F, Feenstra R: The surgical management of chronic hypotony due to uveitis. Eye 19:60-64, 2005
7. Gad K, Singman EL, Nadgir RN, et al: CT in the evaluation of acute injuries of the anterior eye segment. AJR 209:1353-1359, 2017
8. Mönestam E: Frequency of lens dislocation and pseudophacodonesis, 20 years after cataract surgery – a prospective study. Am J Ophthalmol 198:215-222, 2019
9. Raj SM, Vasavada AR, Johar SRK, et al: Post-operative capsular opacification: A review. Int J Biomed Sci 3:237-250, 2007
10. Gaton DD, Mimouni K, Lusky M, et al: Pupillary block following posterior chamber intraocular lens implantation in adults. Br J Ophthalmol 87:1109-1111, 2003
11. Weinreb RN, Aung T, Medeiros FA: The pathophysiology and treatment of Glaucoma. JAMA 311:1901-1911, 2014
12. Schwarz KS, Lee RK, Gedde SJ: Glaucoma drainage implants: A critical comparison of types. Curr Opin Ophthalmol 17:181-189, 2006
13. Schrieber C, Liu Y: Choroidal effusions after glaucoma surgery. Curr Opin Ophthalmol 26:134-142, 2015
14. Al-Torbak AA, Al Shahwan S, Al –Jadaan I, et al: Endophthalmitis associated with the Ahmed glaucoma valve implant. Br J Ophthalmol 89:454-458, 2005
15. Mohamed S, Lai TY: Intraocular gas in vitreoretinal surgery. HKJOphthalmol 14:8-13, 2010
16. Brown DM, Breadsley RM, Fish RH, et al: Long-term stability of circumferential silicone sponge scleral buckling exoplanet. Retina 26:645-649, 2006
17. Abdullah AS, Han S, Qureshi MS, et al: Complications of conventional scleral buckling occurring during and after treatment of rhegmatogenous retinal detachment. J Coll Physicians Surg Pak 20:321-326, 2010
18. Spraul CW, Grossniklaus HE: Vitreous hemorrhage. Serv Ophthalmol 42:3-39, 1997
19. Kubal WS: Imaging of orbital trauma. RadioGraphics 28:1729-1739, 2008
20. Hood MN, Ho VB, Smirniotopoulos JG, et al: Chemical shift: The artifact and clinical tool revisited. RadioGraphics 19:357-371, 1999
21. Barnwell JD, Castillo M: MR imaging of progressive enhancement of a bioceramic orbital prosthesis: An indicator of fibrovascular invasion. AJNR Am J Neuroradiol 32:E8-E9, 2011
22. Jung SK, Cho WK, Paik JS, et al: Long-term surgical outcomes of porous polyethylene orbital implants: A review of 314 cases. Br J Ophthalmol 96:494-498, 2012